

Optical spectral characterization of the the gamma-ray blazars S4 0954+65, TXS 1515-273 and RX J0812.0+0237

J. Becerra González^{1,2*}, J. A. Acosta–Pulido^{1,2†}, W. Boschin^{1,2,3}, R. Clavero^{1,2},

J. Otero–Santos^{1,2}, J. A. Carballo–Bello⁴, L. Domínguez–Palmero^{1,5}

¹*Instituto de Astrofísica de Canarias (IAC), E-38200 La Laguna, Tenerife, Spain*

²*Universidad de La Laguna (ULL), Departamento de Astrofísica, E-38206 La Laguna, Tenerife, Spain*

³*Fundación G. Galilei – INAF (Telescopio Nazionale Galileo), Rambla J. A. Fernández Pérez 7, E-38712 Breña Baja (La Palma), Spain*

⁴*Instituto de Alta Investigación, Universidad de Tarapacá, Casilla 7D, Arica, Chile*

⁵*Isaac Newton Group of Telescopes, Apartado 321, E-38700 Santa Cruz de La Palma, Canary Islands, Spain*

Accepted XXX. Received YYY; in original form ZZZ

ABSTRACT

The study of gamma-ray blazars is usually hindered due to the lack of information on their redshifts and on their low energy photon fields. This information is key to understand the effect on the gamma-ray absorption due to either extragalactic background light and/or intrinsic absorption and emission processes. All this information has also an impact on the determination of the location of the emitting region within the relativistic jets. In this work a new optical spectroscopic characterization is presented for three gamma-ray blazars: S4 0954+65, TXS 1515-273 and RX J0812.0+0237. For all the three targets the redshift determination was successful as well as their classification, belonging all of them to the BL Lac type. For S4 0954+65 ($z=0.3694 \pm 0.0011$) an estimation on the disk, broad line region and torus luminosities was performed based on the observed optical emission lines. The results from this study are compatible with the nature of S4 0954+65 as a transitional blazar. In the case of TXS 1515-273 ($z = 0.1281 \pm 0.0004$), although its optical spectrum is dominated by the continuum emission from the jet, applying the pPXF technique, the stellar population is compatible with an old and metallic population. It is also the case of RX J0812.0+0237 ($z = 0.1721 \pm 0.0002$). Moreover, this work confirms that the optical spectrum from RX J0812.0+0237 is compatible with an extreme blazar classification.

Key words: BL Lacertae objects: general – BL Lacertae objects: individual (S4 0954+65, TXS 1515-273, RX J0812.0+0237) – galaxies: active – galaxies: nuclei

1 INTRODUCTION

Due to geometrical effects, the emission from Active Galactic Nuclei (AGNs) whose relativistic jets points in the direction of the Earth (collectively called blazars) is boosted. Such relativistic jets emit continuum emission through the entire electromagnetic spectrum, from radio to gamma rays. Actually, the extragalactic gamma-ray sky is dominated by the emission from blazars. They constitute the most luminous gamma-ray sources with persistent emission, which together with the relativistic beaming effect, makes possible the detection of distant sources. In order to understand the particles acceleration in relativistic jets, and some of the most energetic processes in the Universe, the study of gamma-ray blazars is crucial. There are still many unknowns associated with such targets, for instance the processes responsible for the high energy emission from blazars, the jet’s structure and the jet’s composition among others (see e.g. [Hovatta & Lindfors 2019](#), and references therein).

The multiwavelength (MWL) spectral energy distribution (SED) from blazars typically displays a double peak structure, where the

first peak is usually centered around the optical to X-ray bands, and the second one within the gamma-ray regime. The emission at low energies can be explained as synchrotron radiation from the relativistic electrons within the jet. While there is consensus on the origin of the low energy emission, different scenarios are considered for the origin of the high energy emission including leptonic and hadronic processes. Different subclasses of blazars can be considered depending on the position of the peaks, the flux ratio between the peak at high and low energies (usually called Compton Dominance -CD-) and their optical spectra. Blazars can be classified as BL Lac objects (BL Lacs) and Flat Spectrum Radio Quasars (FSRQs). BL Lacs typically peaks at higher energies than FSRQs, their CD is relatively small and display nearly featureless optical spectra. In BL Lacs, the optical spectrum is mainly dominated by the continuum emission from the jet, showing only weak emission lines with equivalent widths at rest frame $|EW_{\text{rest}}| < 5\text{\AA}$. On the other hand, FSRQs are typically characterized by a high CD, their SED peaks are located at low frequencies and their optical spectra show strong emission lines ($|EW_{\text{rest}}| > 5\text{\AA}$). Therefore, from the perspective of the study of gamma-ray blazars, their optical spectrum provides crucial information on a) the redshift and b) the existence of external photon

* jbecerra@iac.es

† jose.acosta@iac.es

fields (e.g. the host galaxy or the Broad Line Region -BLR-) which can interact with the jet. The investigation of these two characteristics from three gamma-ray blazars S4 0954+65, TXS 1515-273 and RX J0812.0+0237 is the focus of the present work.

Distant gamma-ray sources, as it is the case of blazars, suffer from absorption on their gamma-ray spectra as the radiation propagates through the Universe. The interaction between gamma rays and the diffuse Extragalactic Background Light (EBL) via pair production is the responsible mechanism for the absorption of the observed gamma-ray spectra (see e.g. [Dwek & Krennrich 2013](#)). In order to infer the intrinsic gamma-ray spectra emitted by distant sources the knowledge of the redshift is essential, as the probability of interaction increases with distance. Moreover, such interaction is also energy dependent, producing not only absorption but also spectral distortion. Unfortunately, the determination of the blazar's redshifts is not an easy task, due to the fact that the continuum emission from their powerful jets outshine the spectral features. For this reason, the characterization of the host galaxy and/or different parts of the AGN cannot be easily observed from blazars. In this work we study the optical spectra from three unknown redshift gamma-ray blazars, providing important information in order to infer both the intrinsic gamma-ray spectra emitted by the target and the EBL imprint (which carries cosmological information).

In addition to the absorption due to the interaction with the EBL, the gamma-ray spectra from blazars can suffer from intrinsic absorption due to the presence of low energy photon fields, as it is the case for the optical emission from the BLR for instance. The characterization of the optical photon field is therefore crucial not only to characterize the possible gamma-ray absorption via pair production, but also to evaluate the possible contribution to the particles acceleration up to gamma rays. Within the leptonic framework, gamma rays are produced via inverse Compton scattering of relativistic electrons with low energy photons e.g. optical photons. Therefore, the characterization of the optical spectrum from blazars will also allow us to estimate the optical external photon fields to the jet in case spectral features are found.

S4 0954+65 was detected in gamma rays by EGRET ([Mukherjee et al. 1995](#)) and later on with *Fermi*-LAT in the high energy range (HE, $E > 100$ MeV) (see [Tanaka et al. 2016](#), and references therein). During a very strong flare detected in almost all wavelengths in 2015, the source was also detected in the very-high-energy (VHE, $E > 100$ GeV) band with the MAGIC telescopes ([MAGIC Collaboration et al. 2018](#)). The redshift and classification of this source are still under debate. The first tentative redshift estimation was $z = 0.368 \pm 0.004$ by [Lawrence et al. \(1986\)](#), based on the preliminary identification of the [O III] emission lines and Mg b absorption feature. Later on, [Lawrence et al. \(1996\)](#) firmly established the redshift as $z=0.3668$ inferred from the identification of [O II], [O III] and $H\alpha$ emission lines. Meanwhile, [Stickel et al. \(1993\)](#) also confirmed the redshift but based on a different set of spectral features, Ca H&K absorption doublet and a very weak [O II] emission feature. Due to the fact that both redshift estimates are derived from a different set of spectral features, new observations were carried out using the 10.4 m Gran Telescopio de Canarias (GTC) by [Landoni et al. \(2015\)](#) aiming to confirm it. This new high signal-to-noise spectral observations taken in 2015 resulted in a featureless spectrum and a lower limit of $z \geq 0.45$ was derived. Therefore, these contradictory results keep still the redshift of S4 0954+65 under debate.

In addition to the redshift, the classification of S4 0954+65 is also controversial. Different authors have classified it as a BL Lac and a FSRQ type target, even it has been classified as a possible transitional blazar between these two categories (see [Abdollahi et al.](#)

[2020](#), and references therein). On the one hand, the target displays weak emission lines or lack of emission lines as later reported. On the other hand, the MWL SED displays a high CD and actually, the standard Synchrotron Self Compton (SSC, [Maraschi et al. 1992](#)) models which typically describe BL Lac objects do not provide a successful approach. Instead, an external field is needed in addition to the SSC in order to explain the SED which shows a SED distribution more similar to FSRQs than BL Lacs ([Tanaka et al. 2016](#); [MAGIC Collaboration et al. 2018](#)). New optical spectroscopic observations are used in this work to investigate the properties of the source.

TXS 1515-273 is a gamma-ray blazar detected in the HE band by *Fermi*-LAT (see e.g. [Abdollahi et al. 2020](#)), classified as a BL Lac. During a flaring state in February 2019, the source was detected in the VHE band with the MAGIC telescopes ([Mirzoyan 2019](#)). The only indication on its redshift comes from the photometric upper limit $z < 1.1$ from [Kaur et al. \(2018\)](#). Optical spectroscopic observations on this object have also been carried out by [Goldoni et al. in prep.](#)

RX J0812.0+0237 is classified as a BL Lac gamma-ray blazar in the 4FGL catalog ([Abdollahi et al. 2020](#)). The source is also a VHE candidate contained in the 2WHSP catalog (2WHSP J081201.7+023732, [Chang et al. 2017](#)). Although the synchrotron peak reported in the 2WHSP catalog is only $10^{-11.6}$ Hz based mainly in the lack of X-ray observations, its MWL SED shows a clear hint of the host galaxy. This fact points to the possibility that RX J0812.0+0237 is a candidate for an extreme blazar. Such extreme blazars (usually name EHBL), are blazars whose SED peaks are located at higher frequencies/energies in comparison with the typical SEDs display by blazars (see e.g. [Biteau et al. 2020](#); [Becerra González et al. 2020](#)). EHBLs are very interesting targets to be explored in the VHE regime as their emission budget is dominated by the VHE emission. Moreover, due to the fact that their emission peaks are located at higher energies than usual, the host galaxy is unveiled in optical. This fact allows us to derive their redshift from the spectral optical features displayed by their host galaxy and characterize its optical emission.

This paper is structured in four sections. In Sec. 2 the observations and data reduction procedures are detailed for the different data samples. The results for each individual target under study in this work are presented in Sec. 3. Finally, the conclusions derived from this work are summarised in Sec. 4.

2 OBSERVATIONS AND DATA REDUCTION

The optical observations presented in this work were carried out with three different telescopes at Roque de los Muchachos observatory located in the Canary island of La Palma. S4 0954+65 was observed during several epochs involving different states of the source using the 3.58 m Telescopio Nazionale Galileo (TNG). For TXS 1515-273 and RX J0812.0+0237 a single observation for each target was performed using the 2.5 m Nordic Optical Telescope (NOT) and the 4.2 m William Herschel Telescope (WHT), respectively. Standard calibration observations for bias, flat field and calibration lamps were also taken during the same night for each of the target observations.

The data were reduced¹ following the standard procedures for bias subtraction and flat-field correction. The sky lines were subtracted averaging the sky spectrum as observed adjacent to the target. The spectra were flux calibrated using spectrophotometric standards taken

¹ IRAF standard packages were used for the different reduction tasks through this work.

after the target observations using the same configuration. Afterwards, the target spectra were corrected for telluric absorption using the task *telluric* available within IRAF packages. The telluric correction was derived from the spectrophotometric standard spectrum, after normalization of the continuum by a smooth function (polynomial). The stellar atmosphere absorption features were masked. We checked for artifacts introduced by the telluric correction by comparison with the atmospheric transmission curves provided by the ESO SkyCalc tool (Noll et al. 2012). Finally, the spectra were corrected using the IRAF task *deredden* for interstellar reddening with the A_V values provided by the NED database (Schlafly & Finkbeiner 2011) and the extinction curve by Cardelli et al. (1989).

The details on the observations and analyses for each target are provided below. In particular, the observation setup for each target and the telescope used in this work are given.

2.1 S4 0954+65

The observations of S4 0954+65 were carried out using the DOLORES (Device Optimized for the LOw RESolution) spectrograph at TNG in long slit configuration. Six observations were carried out using the LRB grism, the details of each observation can be found in Table 1. The He and Hg+Ne calibration lamps were used to calibrate the spectra in wavelength using the same instrumental setup as for the observation of the target and the calibration star.

The flux calibration was performed by applying an spectral response function determined after combining the observations of the spectrophotometric standard stars taken on different nights (see Table 1). This procedure was preferred to avoid introducing systematic differences coming for the use of different spectrophotometric standards. Each spectrum was previously corrected for atmospheric extinction using the extinction curve available for the observatory². In order to confirm the absolute flux scale, each spectrum was rescaled with the *R*-band photometry obtained from the light-curve presented in MAGIC Collaboration et al. (2018) for all dates, except for the 2015 Dec 12 which was taken from Las Cumbres Observatory Global Telescope Network archive (Brown et al. 2013). Finally, the spectra are corrected for interstellar reddening using a value $A_V = 0.328$.

2.2 TXS 1515-273

The spectrum of TXS 1515-273 was observed with the Alhambra Faint Object Spectrograph and Camera (ALFOSC) at NOT. The observations were carried out in long slit configuration using the grism #4 and 1" slit width yielding a resolution $R=357$ at 5500\AA . The observation was performed on 2019 May 7 (starting time MJD 58610.00) for a total of 1 h divided in 3 exposures of 1200 s each. During the observation the seeing was pretty stable from 0.9" to 1.0". Due to visibility constraints from the northern hemisphere, the target was observed at a high airmass of 2.02 at the beginning of the first exposure up to 1.86 at the beginning of the last exposure. Right after the observation of the target, an exposure of the calibration arc of He+Ne was observed using the same instrumental configuration. The flux calibration was performed with the calibration star HD 93521 (Oke 1990) observed with the same instrumental setup as for the target. The telluric absorption features were removed using the spectrum of HD 93521 as a template. Finally, the combined spectrum was corrected for interstellar reddening using $A_V = 0.646$.

² http://www.ing.iac.es/Astronomy/observing/manuals/ps/tech_notes/tn031.pdf

The absolute flux level was checked using photometry obtained in *R*-band with the Kungliga Vetenskapsakademien (KVA) telescope. The data are analyzed using the differential photometry method described by Nilsson et al. (2018). The KVA photometric observation was performed on 2019 May 6 (MJD 58609.95), ~ 1 h before of our spectroscopic observations with NOT, yielding an *R*-band magnitude $\simeq 15.9$ (KVA team private communication). After extinction correction, our flux calibrated spectrum and the photometry agrees within a 5% uncertainty.

2.3 RX J0812.0+0237

The optical spectrum of RX J0812.0+0237 was obtained using ACAM (Auxiliary-port CAMera) at WHT on 2017 October 20 (starting time MJD 58046.24). The target was observed for a total of 300 s, 3 exposures of 100 s each. The airmass at the beginning of the observation was 1.23. A 400 lines/mm transmission VPH (Volume Phase Holographic) grating is mounted in ACAM and a 1" long slit was used for the experimental design. This configuration yields a resolution $R=450$ at 5500\AA . The seeing during the observation of the target was good, oscillating between 0.6" and 1". The flux calibration was based on the star SP 0236+052, observed with the same configuration used for the target observation. The wavelength calibration arc lamps were CuNe+CuAr. The spectrum was also corrected for telluric absorption using a template derived from the standard star spectrum, which was obtained at airmass 1.088. The spectrum was corrected for interstellar reddening using $A_V = 0.073$.

3 RESULTS

The analysis of the optical spectra from the three gamma-ray sources presented in this work yields to the determination of their redshifts. The uncertainties of the measured redshifts are estimated by performing Montecarlo simulations of the observed spectrum with the uncertainty estimated from the RMS of the continuum. The spectral features of the simulated spectra are then fitted again with a Gaussian function and the error is obtained from the resulting distribution of centroids. All of them are inferred from the detection of emission and/or absorption spectral features. While emission lines are found in the spectra from S4 0954+65 and TXS 1515-273, the spectrum from RX J0812.0+0237 is dominated by stellar absorption features. It is consistent with the fact that RX J0812.0+0237 is classified as an extreme gamma-ray blazar, whose synchrotron emission peak is shifted to higher energies w.r.t. other types of blazars, and therefore unveiling the emission from the host galaxy (typically characterized by absorption features). The detailed results on each target are discussed in the following subsections.

3.1 S4 0954+65

The flux calibrated spectra from S4 0954+65 taken during different states of the source are shown in Fig. 1. The spectra are highly dominated by the continuum emission from the jet, as typically occurs in blazars. It is specially the case during the high state of the source, where it is difficult to identify any spectral feature except for the Na I absorption line from the interstellar medium (IS). However, during the low state of the source when the synchrotron radiation from the jet is lower (see zoom plot from Fig. 1), an emission line is clearly visible at the beginning of the spectrum, identified as Mg II 2800 \AA . In addition, [OIII] 5007 \AA can be also detected and a very weak [O II] 3727 \AA emission line seems to be present in the

Date	MJD	Exposure	Slit	Airmass	Star	Seeing (star)	R@5500 Å	S/N
2015-02-24	57077.02	3x500 s	1.0"	1.25	Hiltner 600	2.3"-2.5 (2.7")	550	84
2015-04-23	57135.88	1x1000 s	1.0"	1.25	BD+75325	0.8" (0.9")	550	86
2015-05-19	57161.89	1x1800 s	1.5"	1.33	Feige 66	0.7" (1.4")	367	105
2015-05-21	57163.90	3x1200 s	2.0"	1.35	Feige 34	0.6" (0.6")	275	160
2015-06-27	57200.89	1x1800 s	1.5"	1.75	Feige 66	1.9" (1.7")	367	113
2015-12-12	57368.13	1x900 s	1.5"	1.40	Hiltner 600	0.9" (0.8")	367	128

Table 1. Information on the long slit spectroscopic observations of S4 0954+65 carried out at TNG with DOLORES using the LRB grism. The MJD date and the airmass refers to the start of the observation. The column named star refers to the flux calibration star observed for each target observation. The seeing value is given for the target observation, followed by that of the calibration star in brackets. The resolution given in this table refers to the value given by the slit width. The S/N of the spectrum calculated in the range 4100–4600 Å is given in the last column. The best S/N is achieved on 2015 May 21, due to the fact that it was taken with the longest exposure and the best seeing conditions.

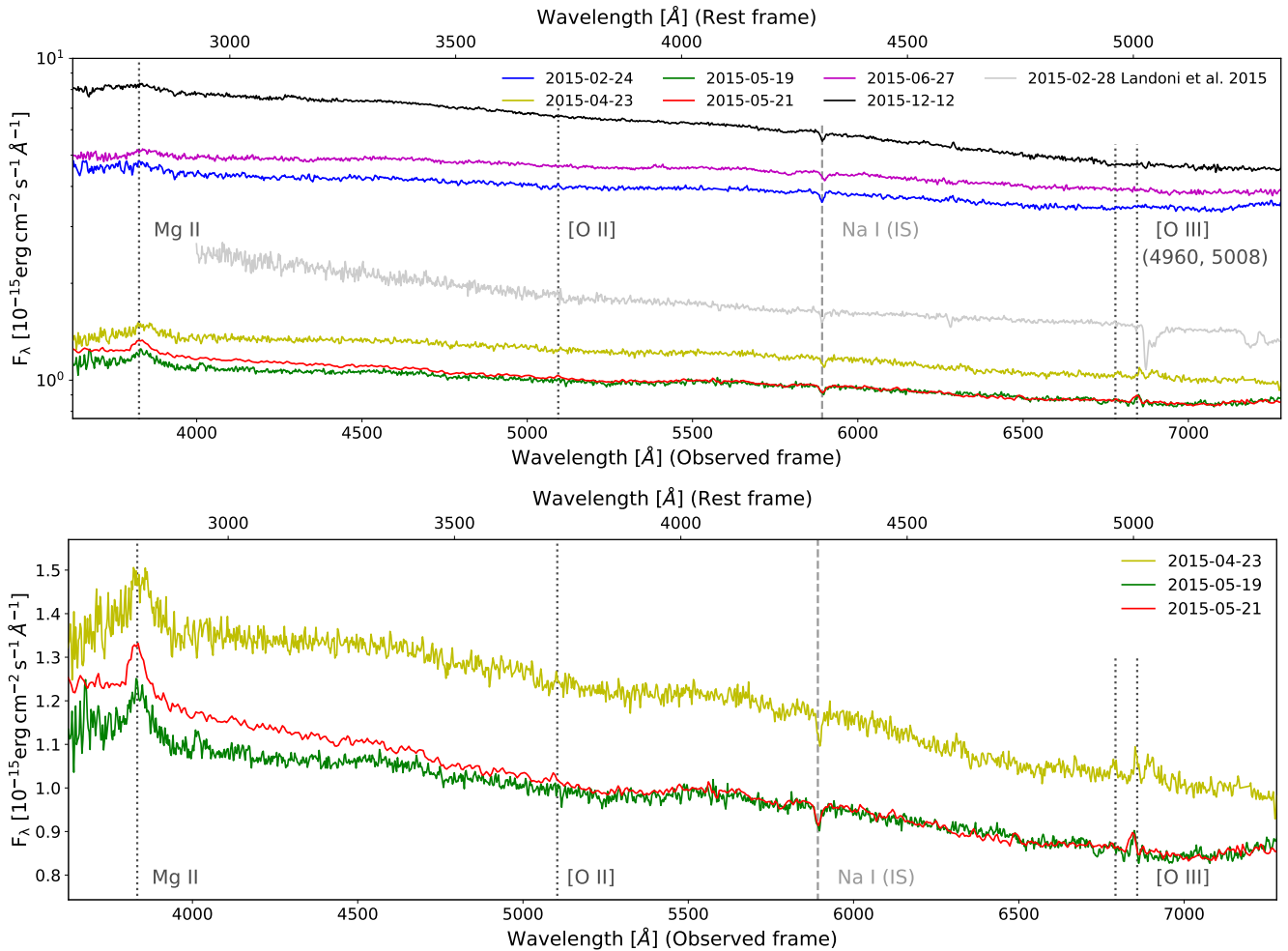


Figure 1. S4 0954+65 optical spectrum and the zoom of the spectra taken during the low state of the source where the spectral features can be identified. The spectrum from [Landoni et al. \(2015\)](#) is also shown in grey for comparison purposes. All spectra, including the archival one, are corrected calibrated using photometric observations and for interstellar reddening.

spectra. These features are present in the three spectra taken during low flux state of the source, namely during April and May 2015. We perform the calculations below based on the best quality spectrum taken on 2015-05-21 (see S/N ratios in Table 1). The emission line flux measurements were obtained by Gaussian fitting and are reported in Table 2 for that night. The flux of Mg II during other nights was consistent with the reported value, while the other lines show very low S/N ratios and were not measured. There is no sign of stellar

absorption features in any of the obtained spectra of S4 0954+65, which indicates that the host galaxy light is completely outshined by the AGN contribution.

We obtained consistent redshift estimates based on the strongest emission lines detected on the spectra taken on 2015-05-21. Thus, the estimated redshift of S4 0954+65 is $z=0.3694 \pm 0.0011$ is derived from the Mg II line, and the values $z=0.3667 \pm 0.0003$ and $z=0.3671 \pm 0.0003$ are derived from the lines [OIII] and [OII], respectively.

[Emission Lines Measurements S4 0954+65]

Line ID	Center [Å]	EW _{rest} [Å]	Flux	Lum.
Mg II	3833.6±2.7	-4.09±0.37	68±7	31.9±0.07
[OII]3727	5095.0±1.3	-0.47±0.09	3.8±0.6	1.79±0.26
[OIII]5007	6842.6±1.7	-0.69±0.15	8.8±1.2	4.14±0.6

Table 2. Parametrization of the optical emission lines from S4 0954+65. Only the observations performed on 2015-05-21 are considered as it corresponds to the higher S/N spectrum, being the emission lines better characterized. [O III] in this table only refers to the line at 5008.24 Å at rest frame. The flux is given in 10^{-16} erg cm $^{-2}$ s $^{-1}$ units, while the luminosity is given in 10^{41} erg s $^{-1}$.

Therefore, our results confirm the previous redshift estimates from Lawrence et al. (1986, 1996); Stickel et al. (1993). Hence, the redshift lower limit of $z \geq 0.45$ derived more recently by Landoni et al. (2015) is ruled out based on the results on this work. As shown in Fig. 1, the redshift lower limit was estimated based on a featureless spectrum while the source was still in flaring state, moreover the spectrum has a limited S/N of 30 (calculated in the range 4100-4600 Å) in comparison with the higher S/N spectra presented in this work (see Table 1).

The luminosity of the line [OIII] in S4 0954+65 is among the less luminous QSO contained in the SDSS (Shen et al. 2011). Furthermore, the line ratio [OIII]/[OII]=2.3 indicates high ionization gas, whose excitation is likely due to photoionization by the nuclear emission (Moy & Rocca-Volmerange 2002).

Regarding the classification of the source, according to the EW at rest frame measure for the Mg II line, it is < 5 Å (see Table 2) and therefore, the source can be classified as a BL Lac object. However, it is close to the limit of 5 Å, possibly being consistent with the existence of a weak BLR. From the MWL SEDs of S4 0954+65 reported in Tanaka et al. (2016); MAGIC Collaboration et al. (2018), the high CD reported in both works, clearly demonstrates that standard one-zone SSC models fail to explain the MWL emission from the source. Indeed, in order to successfully explain the MWL emission from S4 0954+65 external photon fields are invoked in addition to the SSC emission. In particular, to avoid absorption of gamma rays (specially in the VHE band) within a possible BLR, the authors assume a location of the emitting region closer to a possible IR torus and uses such external photon field as the possible source of radiation external to the jet. Therefore, this source could be classified as a transitional blazar: on one hand it displays relatively weak emission lines and on the other hand, the CD is similar to the one usually present in FSRQs (requesting the same type of theoretical modeling including external photon fields).

From the optical spectra presented in this work we can derive the expected luminosity of the BLR and the torus in order to compare it with the photon field needed to explain its MWL SED. On the first place the luminosity of the BLR can be estimated as proposed by Celotti et al. (1997), $L_{\text{BLR}} \approx 5.6 L_{\text{Ly}\alpha}$. Since the only broad line detected in our spectra is Mg II, we use the average relative emission line ratio between Mg II and Ly α as 34% as reported by Francis et al. (1991). Therefore, the relation between the luminosity of the BLR and the luminosity of the Mg II emission line should be $L_{\text{BLR}} \approx 16.5 L_{\text{MgII}} \approx 5.3 \cdot 10^{43}$ erg s $^{-1}$. From this estimation and assuming a standard covering factor of the BLR of $f_{\text{covBLR}} = 0.1$ (maximum value found is 0.15 by Smith et al. 1981), an estimation of the disk luminosity can be derived as $L_{\text{disk}} \approx 1/f_{\text{covBLR}} \cdot L_{\text{BLR}} \approx 5.3 \cdot 10^{44}$ erg s $^{-1}$. The estimated L_{disk} is consistent with the distribution found by Ghisellini et al.

(2014). The IR torus luminosity can also be derived from the disk luminosity, assuming a certain covering factor. The standard values for the covering factor for the torus range from 0.5 to 0.7 according to Calderone et al. (2012). In this work a mean value of 0.6 will be used. Therefore, the torus luminosity for S4 0954+65 is $L_{\text{torus}} = f_{\text{covtorus}} \cdot L_{\text{disk}} \approx 3.2 \cdot 10^{44}$ erg s $^{-1}$. The radius of the IR torus can be inferred as $r_{\text{torus}} \approx 2.5 \cdot 10^{18} [L_{\text{disk}}/(10^{45} \text{ erg s}^{-1})]^{1/2}$ cm $\approx 1.8 \cdot 10^{18}$ cm ≈ 0.6 pc as prescribed by Ghisellini & Tavecchio (2009).

From the MWL SED modeling of S4 0954+65 in MAGIC Collaboration et al. (2018), the assumed physical environment responsible for the external IR photon field are $L_{\text{torus}} = 1.5 \cdot 10^{42}$ erg s $^{-1}$ and $r_{\text{torus}} = 6.1 \cdot 10^{17}$ cm = 0.2 pc. Therefore the assumed IR torus luminosity is more than two orders of magnitude below the luminosity compatible with the observed Mg II emission line in its optical spectrum, while the assumed radius of the torus is around 3 times smaller than the dimension derived in this work. From this results we can conclude that even if the source is classified as a BL Lac object, its optical spectrum is compatible with the existence of an IR torus powerful enough to provide the external photon field required for the production of gamma rays needed to successfully explain its MWL SED.

3.2 TXS 1515-273

The flux calibrated spectrum from TXS 1515-273 is reconstructed with a S/N of 227 in the range 4500-4800 Å (see Fig. 2). Both emission and absorption spectral features can be identified. The list of the spectral features detected together with its parametrization can be found in Table 3. The derived redshift from such spectral features and their identification is $z = 0.1281 \pm 0.0004$, which uncertainty is estimated from the [O II] emission line.

Due to the fact that only weak emission lines have been detected from TXS 1515-273 with small equivalent widths ($EW_{\text{rest}} < 5$ Å), the target can be classified as a BL Lac object. The emission line ratios [OIII]/[OII] ≈ 0.5 and [NII]/H $\alpha \approx 1.7$ indicate a very low ionization level of the line-emitting gas, as observed in LINERS or Low-Luminosity AGNs (LLAGNs). The most plausible excitation mechanism in this case is a combination of photoionization and shocks (Moy & Rocca-Volmerange 2002). The luminosity of the line [OIII] is relatively low ($\log(L_{\text{um}}([OIII])) = 40.7$) which is compatible with the nucleus being a LLAGNs. There are predictions that at low nuclear luminosities the BLR should disappear (Elitzur & Ho 2009), which is consistent with the non-detection of broad lines in the spectra of TXS 1515-273.

The presence of weak stellar absorption features in the spectrum of TXS 1515-273 suggests that the stellar population contribution is significantly diluted by the nuclear non-stellar continuum. In order to uncover the underlying stellar population we have applied the penalized pixel fitting technique (pPXF) (Cappellari 2017). We have used the same set of synthesis models as in Becerra González et al. (2020), where a detailed description can be found. The regions showing emission lines and the NaI interstellar absorption feature were masked prior to the modelling. Given the dominance of the non-stellar contribution we model the observed optical spectrum by adding to the stellar templates a second order Legendre polynomial (in a $\log(\lambda)$ scale), which permits to improve the fit without varying the template continuum shape. The addition of this polynomial component mimics the commonly observed power law component and accounts for the likely featureless contribution from the active nucleus. The mass-weighted age and metallicity of the best fitting models indicates a very old ($< \log(\text{Age}) > = 1.112 \pm 0.002$ Gyr) and metallic ($< [M/H] > = 0.25 \pm 0.04$) stellar population.

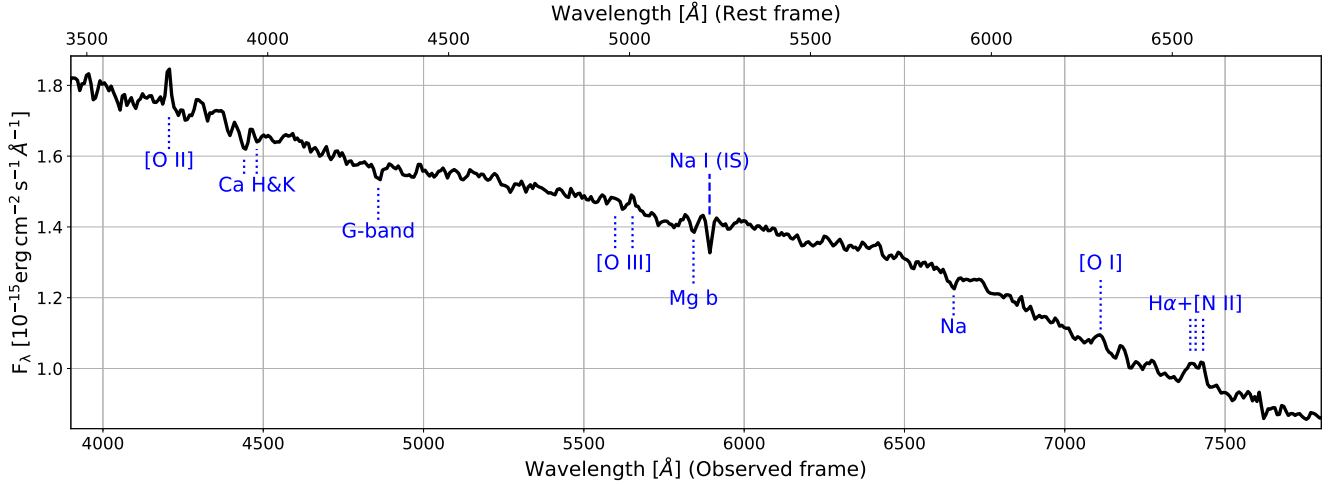


Figure 2. TXS 1515-273 optical spectrum obtained at NOT on 2019 May 7. The detected spectral features are consistent with a redshift value of $z = 0.1281 \pm 0.0004$. See text for details.

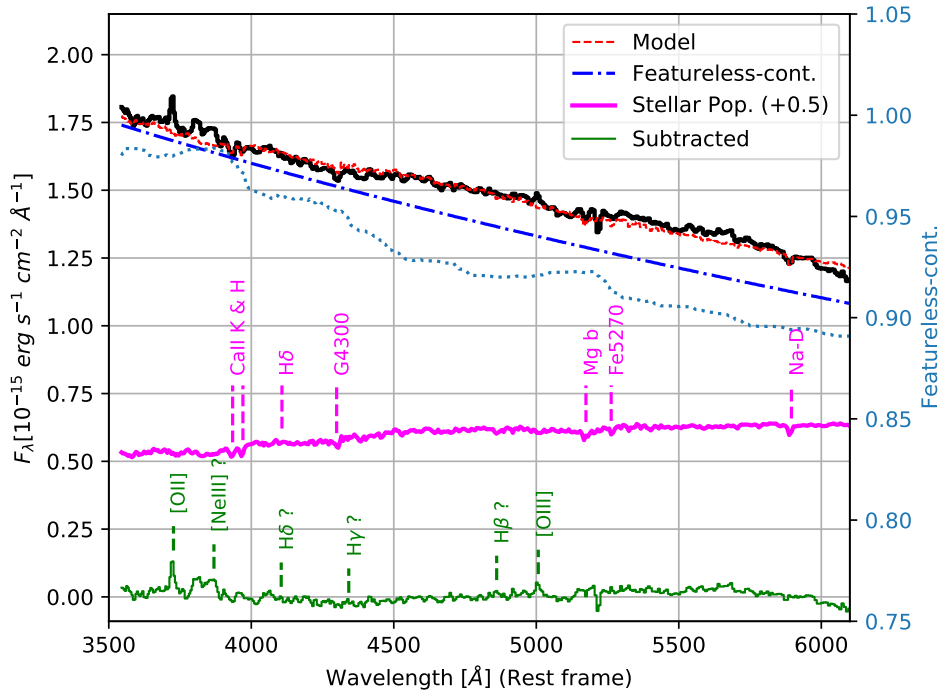


Figure 3. Optical spectra of TXS 1515-273 (black) and best fit model (red) obtained using pPXF, which includes a featureless continuum (blue) and the stellar population contribution (magenta), adding an offset of 0.5 flux units for representation purpose. The subtraction of the model to the observed spectra is shown at residual level (green line). It can be noticed that the stellar absorption lines are relatively well reproduced and the emission lines emerges. Absorption and emission spectral features are marked in the figure. The right y-axis refers to the contribution of the featureless continuum to the observed spectrum (dotted blue line).

Urry et al. (2000) claimed that BL Lac objects are hosted by giant elliptical galaxies showing a narrow distribution of M_R^{host} , independently of the nuclear luminosity. The contribution of the stellar population from the host galaxy can be obtained from the pPXF modelling. We estimate a host contribution in the range 15-20% (see Fig. 3) to the brightness observed in the R-band ($m_R^{host} = 15.99$). Thus the apparent magnitude in R of the stellar population is in the range $m_R^{host} = 17.25 - 17.54$, after interstellar reddening correction. This value refers to the contribution included within the slit. We

estimate about 1.3 mags due to slit losses due to the extension of the host galaxy assuming a de Vaucouleurs profile (Sersic $n=4$) for $r_{eff} = 7$ kpc (compatible with Urry et al. 2000, in their Fig. 3 at the estimated redshift), corresponding to $r_{eff} = 2.97''$. From these values and the derived redshift we can estimate the absolute magnitude of the host galaxy, which results in M_R^{host} from -22.7 to -22.9 , which is slightly above the peak of the brightness distribution of BL Lac host absolute magnitudes according to Shaw et al. (2013), but compatible within the uncertainties given in that work ($M_R^{host} = -22.5 \pm 0.5$).

[Spectral Features TXS 1515-273]

Line ID	Center [Å]	EW _{rest} [Å]	Flux	Lum.
[OII]3727	4204.3±1.5	-1.24±0.27	2.12±0.36	9.25±1.58
Ca K	4440±4	1.1±0.4
Ca H	4484±7	0.6±0.4
G-band	4859±1	0.53±0.09
[OIII]5007	5651±4	-0.89±0.27	1.16±0.31	5.08±1.34
Mg b	5842±5	0.74±0.3
Na	6651±4	0.97±0.18
[OI]6300	7110±5	-1.15±0.27	1.17±0.31	5.13±1.36
H α *	7401±4	-3.37±0.53	1.06±0.50	4.65±2.18
[NII]6584*	7424±4	-3.37±0.53	1.81±0.41	7.94±1.78

Table 3. Spectral features detected in the optical spectrum from TXS 1515-273. The flux is given in 10^{-15} erg cm $^{-2}$ s $^{-1}$ units, while the luminosity is given in 10^{40} erg s $^{-1}$. Notes: *The center and width of the lines [NII]6584,6584 are linked to the values corresponding to H α . The line flux ratio [NII]6584/6548 is kept fixed to the theoretical value 3.

[Absorption Features RX J0812.0+0237]

Line ID	Center [Å]	EW _{rest} [Å]
Ca K	4615*	3.4*
Ca H	4652*	4.1*
Mg b	6064.9*	4.7*
Na	6906.1±1.4	4.6±0.46

Table 4. Absorption lines detected in the optical spectrum from RX J0812.0+0237. * These features have been measured in the smoothed spectra, hence uncertainty estimation cannot be done using our method based on Montereal simulations.

The derived values indicate that the host galaxy could be a luminous bright elliptical galaxy.

3.3 RX J0812.0+0237

The flux calibrated optical spectrum from RX J0812.0+0237 is shown in Fig. 4. Although the S/N is only 17 (calculated in the range 5000-5500 Å) it can be clearly appreciated that the spectrum is dominated by the emission from the host galaxy, and therefore, the absorption features dominate the spectrum. The different absorption lines identified are listed in Table 4. The corresponding estimated redshift is $z = 0.1721 \pm 0.0002$, based on the Na absorption line.

The observed spectrum from RX J0812.0+0237 is compatible with the classification as extreme blazar from the 2WHSP catalog (Chang et al. 2017), as its optical emission is dominated by the host galaxy and not the emission from the relativistic jet. This fact indicates that the emission peaks from the MWL SED are located at high energies, unveiling the emission from the host galaxy instead of outshining it as it is commonly observed in less energetic blazars.

Given the high noise value observed in the spectrum we have applied a Gaussian filter (FWHM=4 pixels, as corresponding to the slit width). We have tried to model the stellar population using pPXF to reproduce the smoothed optical spectrum of RX J0812.0+0237. We cannot firmly rely on the resulting spectral shape given the limited S/N ratio of our spectrum. In order to improve the modelling we use a multiplicative polynomial function to adjust the continuum shape of the template to the measured spectrum. The best results were obtained

with an order 3 polynomial which accounts for deviations of the spectral shape of $\pm 10\%$ with respect to the synthesis templates. The best fit is obtained for a model with weighted-mass age and metallicity values of $\langle \log(\text{Age}) \rangle = 1.059 \pm 0.003$ Gyr and $\langle [M/H] \rangle = 0.183 \pm 0.011$, respectively.

Our model fit confirms that the optical emission from RX J0812.0+0237 is completely dominated by the host stellar population. Hence, the host galaxy luminosity at the R -band can be estimated from the photometry reported in the SDSS. We have used the value $r = 16.85$ obtained from the cmodel³ and take it as the same as R band. Note that the magnitude reported as PSF modelling ($r = 17.629$) is in better agreement with the flux level of the observed spectrum. This results can be explained if the host galaxy is resolved for seeing limited observations, which is compatible with the difference between cmodel and PSF values reported in SDSS archive. The luminosity distance was computed using the cosmological calculator by Wright (2006) using our redshift estimation. Thus the host absolute magnitude in the R -band is ~ -22.8 , which is close to the maximum of the BL Lacs host brightness distribution as found by Shaw et al. (2013). The derived value is consistent with the host galaxy of RX J0812.0+0237 being a large elliptical galaxy, as expected for a bright high-energy BL Lac.

4 CONCLUSIONS

In this work, we present the redshift estimation of three gamma-ray blazars whose distance was previously either unknown or under debate. Moreover, the optical spectroscopic information from those sources are also used to classify them. The individual conclusions from the study of each target are:

- S4 0954+65: a solid redshift determination of $z = 0.3694 \pm 0.0011$ is established for this target, confirming the historical measurements from Lawrence et al. (1986, 1996); Stickel et al. (1993) and ruling out the lower limit of $z \geq 0.45$ derived by Landoni et al. (2015) on February 2015. This work shows the importance of the state of the source during the optical spectroscopic observations. When the source is in high state the continuum emission from relativistic jets can easily outshine the spectral features, which is the main reason for the debate on the redshift of this source. During the observations performed by Landoni et al. (2015) the source displayed a higher flux (almost double) than the spectra in low state presented in this work and the historical observations. This makes more difficult to detect the weak [O III] very close to the telluric absorption features (which were not corrected in Landoni et al. 2015). In addition, the GTC spectrum used to derive the redshift lower limit starts at 4000 Å, while the strong emission line Mg II detected in the TNG spectrum is located at ~ 3830 Å (see Fig. 1). With this work, we can also confirm the classification of S4 0954+65 as a BL Lac object, but close to the limit and therefore, it seems to confirm that the target could be a transitional object showing characteristics from both BL Lacs and FSRQs. From the observed Mg II emission line the luminosity of the disk, BLR and torus have been derived under certain commonly used assumption for the covering factors. The results demonstrate that the observed optical spectrum is compatible with the existence of a torus luminous enough to provide the IR external photon field needed for the production of gamma rays as required by the high CD MWL SED.

³ <https://www.sdss.org/dr12/algorithms/magnitudes/>

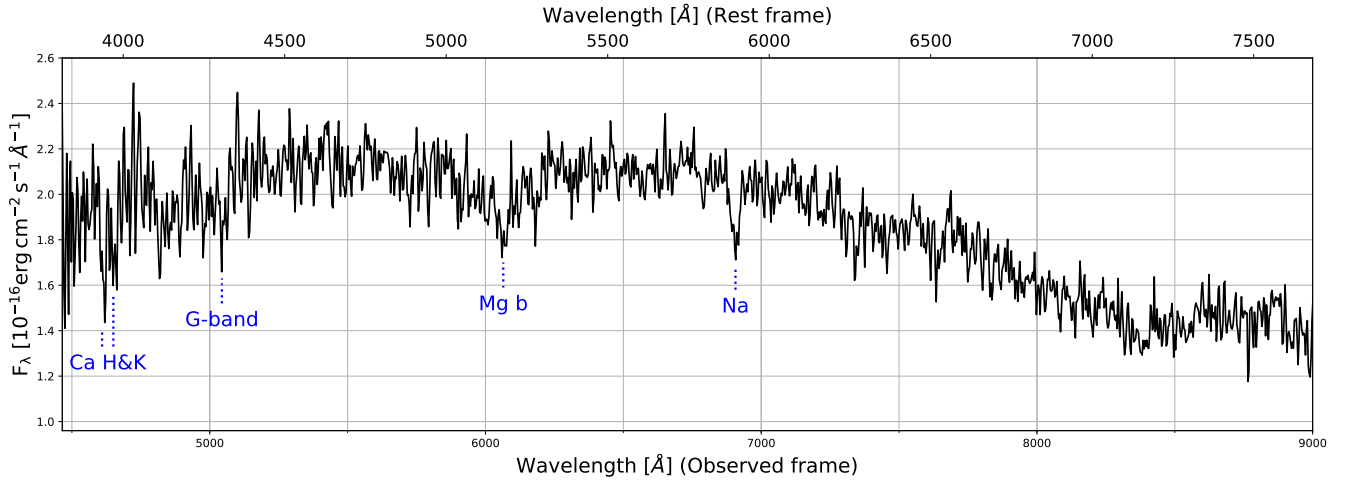


Figure 4. RX J0812.0+0237 optical spectrum observed at WHT on 2017 October 20. Based on the detection of its absorption spectral features, a redshift of $z = 0.1721 \pm 0.0002$ is derived. See text for details.

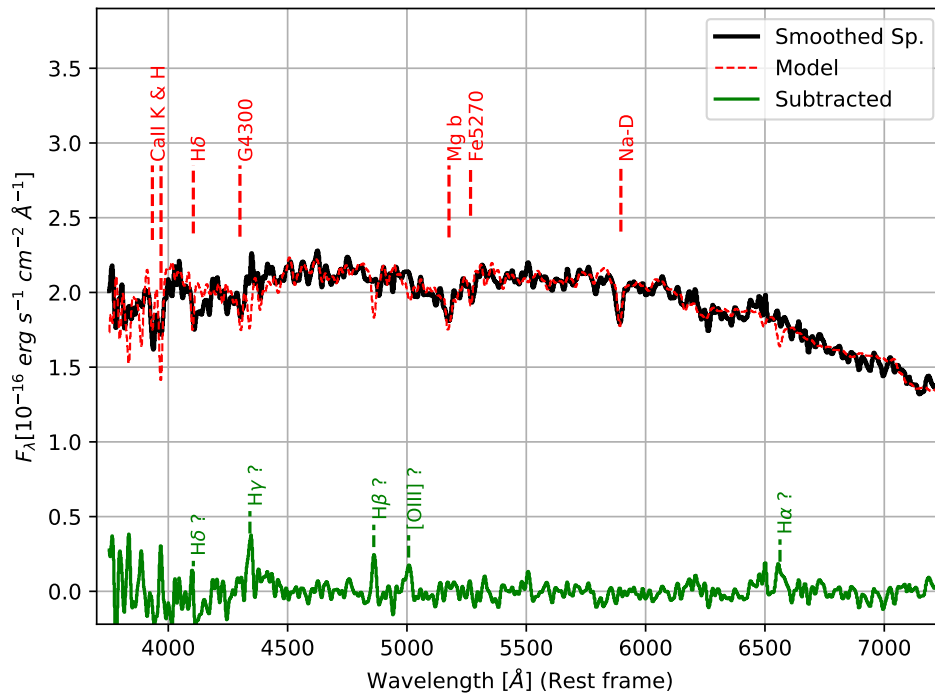


Figure 5. Optical spectra of RX J0812.0+0237 (black) and best fit model (red) obtained using pPXF. The subtraction of the model to the observed spectra is shown at residual level (green line). It can be noticed that the stellar absorption lines are relatively well reproduced and possible emission lines emerge. Absorption and emission spectral features are marked in the figure.

- **TXS 1515-273:** the redshift determination of the source as $z = 0.1281 \pm 0.0004$ is presented in this work, being this information crucial for further studies of its gamma-ray emission. The source classification as a BL Lac object is confirmed based on the weak optical emission lines detected. While its optical spectrum is dominated by the continuum emission from the jet, the weak underlying stellar population has been modeled using the pPXF technique. The best fit found yields an old and metallic stellar population with $\langle \log(\text{Age}) \rangle = 1.112 \pm 0.002$ Gyr and $\langle [M/H] \rangle = 0.25 \pm 0.04$. The absolute magnitude of the host galaxy resulted in M_R^{host} from -22.7 to -22.9 , comparable with the

peak of the luminosity distribution of the BL Lac sample from [Shaw et al. \(2013\)](#).

- **RX J0812.0+0237:** from the spectral shape and the detection of absorption features we can confirm that the spectrum is dominated by its host galaxy, as typically occurs in extreme blazars. Therefore, the results presented in this work are consistent with the classification of the source as a 2WHSP target. Its redshift can be firmly established for the first time as $z = 0.1721 \pm 0.0002$ thanks to the identification of a few optical spectral features. The stellar population has been modeled with pPXF, yielding $\langle \log(\text{Age}) \rangle = 1.059 \pm 0.003$ Gyr and $\langle [M/H] \rangle = 0.183 \pm 0.011$. The analysis results in an absolute

magnitude of the host galaxy of RX J0812.0+0237 $M_R^{host} \sim -22.8$, again close to the average magnitude found by Shaw et al. (2013) for a BL Lac sample.

All this new information is essential for the study of the intrinsic characteristics of the three studied gamma-ray BL Lac objects, since the redshift is a key information to determine the EBL absorption suffered by the gamma-ray spectrum (specially in the VHE band). Moreover, the classification of the target and the study of the characteristics of a possible BLR is also important information for the modeling of their MWL SEDs. In addition to the use of our results for the study of these sources within the current gamma-ray context, they will be better studied using the capabilities of the next generation of Cherenkov telescopes, the Cherenkov Telescope Array (CTA) currently under construction.

5 ACKNOWLEDGEMENTS

We thank Paolo Goldoni, Roopesh Ojha and Tapio Pursimo for useful discussions. We thank Elina Lindfors and the KVA team for providing information on the optical magnitude of TXS 1515-273. JBG acknowledges the support of the Viera y Clavijo program funded by ACIISI and ULL. JBG and JAP acknowledges financial support from the Spanish Ministry of Economy and Competitiveness (MINECO) under the 2015 Severo Ochoa Program MINECO SEV-2015-0548. JOS thanks the support from grant FPI-SO from the Spanish Ministry of Economy and Competitiveness (MINECO) (research project SEV-2015-0548-17-3 and predoctoral contract BES-2017-082171).

Based on observations made with the Italian Telescopio Nazionale Galileo, the Nordic Optical Telescope and the William Herschel Telescope. These telescopes are located in the Spanish Observatorio del Roque de los Muchachos of the Instituto de Astrofísica de Canarias, and are operated by the Fundación Galileo Galilei of the INAF (Istituto Nazionale di Astrofisica), the Nordic Optical Telescope Scientific Association and the Isaac Newton Group, respectively.

6 DATA AVAILABILITY

The data reported in this work are available at the archival databases from the different telescopes used: TNG, WHT and NOT.

REFERENCES

- Abdollahi S., et al., 2020, *ApJS*, 247, 33
 Becerra González J., Acosta-Pulido J. A., Clavero R., 2020, *MNRAS*, 494, 6036
 Biseau J., et al., 2020, *Nature Astronomy*, 4, 124
 Brown T. M., et al., 2013, *PASP*, 125, 1031
 Calderone G., Sbarrato T., Ghisellini G., 2012, *MNRAS*, 425, L41
 Cappellari M., 2017, *MNRAS*, 466, 798
 Cardelli J. A., Clayton G. C., Mathis J. S., 1989, *ApJ*, 345, 245
 Celotti A., Padovani P., Ghisellini G., 1997, *MNRAS*, 286, 415
 Chang Y. L., Arsioli B., Giommi P., Padovani P., 2017, *A&A*, 598, A17
 Dwek E., Krennrich F., 2013, *Astroparticle Physics*, 43, 112
 Elitzur M., Ho L. C., 2009, *ApJ*, 701, L91
 Francis P. J., Hewett P. C., Foltz C. B., Chaffee F. H., Weymann R. J., Morris S. L., 1991, *ApJ*, 373, 465
 Ghisellini G., Tavecchio F., 2009, *MNRAS*, 397, 985
 Ghisellini G., Tavecchio F., Maraschi L., Celotti A., Sbarrato T., 2014, *Nature*, 515, 376
 Hovatta T., Lindfors E., 2019, *New Astron. Rev.*, 87, 101541

- Kaur A., Rau A., Ajello M., Domínguez A., Paliya V. S., Greiner J., Hartmann D. H., Schady P., 2018, *ApJ*, 859, 80
 Landoni M., Falomo R., Treves A., Scarpa R., Reverte Payá D., 2015, *AJ*, 150, 181
 Lawrence C. R., Pearson T. J., Readhead A. C. S., Unwin S. C., 1986, *AJ*, 91, 494
 Lawrence C. R., Zucker J. R., Readhead A. C. S., Unwin S. C., Pearson T. J., Xu W., 1996, *ApJS*, 107, 541
 MAGIC Collaboration et al., 2018, *A&A*, 617, A30
 Maraschi L., Ghisellini G., Celotti A., 1992, *ApJ*, 397, L5
 Mirzoyan R., 2019, The Astronomer's Telegram, 12538, 1
 Moy E., Rocca-Volmerange B., 2002, *A&A*, 383, 46
 Mukherjee R., et al., 1995, *ApJ*, 445, 189
 Nilsson K., et al., 2018, *A&A*, 620, A185
 Noll S., Kausch W., Barden M., Jones A. M., Szyszka C., Kimeswenger S., Vinther J., 2012, *A&A*, 543, A92
 Oke J. B., 1990, *AJ*, 99, 1621
 Schlafly E. F., Finkbeiner D. P., 2011, *ApJ*, 737, 103
 Shaw M. S., et al., 2013, *ApJ*, 764, 135
 Shen Y., et al., 2011, *ApJS*, 194, 45
 Smith M. G., et al., 1981, *MNRAS*, 195, 437
 Stickel M., Fried J. W., Kuehr H., 1993, *A&AS*, 98, 393
 Tanaka Y. T., et al., 2016, *PASJ*, 68, 51
 Urry C. M., Scarpa R., O'Dowd M., Falomo R., Pesce J. E., Treves A., 2000, *ApJ*, 532, 816
 Wright E. L., 2006, *PASP*, 118, 1711

This paper has been typeset from a $\text{\TeX}/\text{\LaTeX}$ file prepared by the author.